X-ray structural studies on elemental liquids under high pressures

2003 J. Phys.: Condens. Matter 15 6085

(http://iopscience.iop.org/0953-8984/15/36/302)

INSTITUTE OF PHYSICS PUBLISHING JOURNAL OF PHYSICS: CONDENSED MATTER

J. Phys.: Condens. Matter **15** (2003) 6085–6103 PII: S0953-8984(03)58273-X

X-ray structural studies on elemental liquids under high pressures

Yoshinori Katayama[1] **and Kazuhiko Tsuji**[2]

[1] Synchrotron Radiation Research Centre, Japan Atomic Energy Research Institute, Kouto 1-1-1, Mikazuki, Sayo, Hyogo 679-5148, Japan
[2] Department of Physics, Faculty of Science and Technology, Keio University, Hiyoshi 3-14-1, Kohoku, Yokohama 223-8522, Japan

E-mail: katayama@spring8.or.jp

Received 14 January 2003, in final form 2 May 2003
Published 29 August 2003
Online at stacks.iop.org/JPhysCM/15/6085

Abstract

X-ray structural studies on several elemental liquids under high pressure are reviewed. Combination of synchrotron radiation sources and large-volume presses enables us to carry out *in situ* structural measurements on liquids at high pressures up to several gigapascals. The measurements have revealed that compressions of liquid alkali metals are almost uniform, whereas those of liquids that have covalent components in bonding are mostly anisotropic. For covalent liquids, the volume dependence of the nearest-neighbour distance deviates from $(V/V_0)^{1/3}$ behaviour (V being the molar volume and V_0 being the molar volume at zero pressure) and changes in coordination play important roles. In some elements, different types of volume dependence of the nearest-neighbour distances are observed in different pressure ranges. This behaviour suggests that the liquid phase can be divided into regions. Although most of the observed structural changes are continuous, a discovery of an abrupt structural change in liquid phosphorus, which is completed over a pressure range of less than 0.05 GPa around 1 GPa and 1050 °C, supports the existence of a first-order liquid–liquid phase transition.

1. Introduction

Recently, there has been increasing interest in the high-pressure behaviour of liquids [1]. To understand the background, we briefly review previous studies on liquids at atmospheric pressure and solids under high pressure.

Structural studies on liquids at atmospheric pressure revealed a wide variety of short-range orders in the liquid state [2]. It was established that the structures of the elements in the liquid state follow characteristic trends [3] reminiscent of the trends among the crystal structures

of the elements [4, 5]. While the liquid structure of many metallic elements is described by a simple hard-sphere-like structure with coordination number of 9–11, that of some metallic elements shows deviations from the simple structure. Elements that have covalent bonds and open-packed crystalline structures, such as three-dimensional network (group IV elements), layer (group V elements) and chain (group VI elements) structures, melt into liquids that are characterized by low coordination numbers. For example, coordination numbers are six for Si and Ge, three for As, six for Sb and two for Se and Te in the liquid state. Covalent characters in the bonding remain in the liquid state for those elements. In fact, these liquids are poor metals or semiconductors. Moreover, molecular solids usually melt into molecular liquids. Structural changes in the liquid state near atmospheric pressure have been explored mainly by temperature dependence and by concentration dependence in alloys. Many interesting observations, such as polymerization of sulfur [6], nonmetal (semiconductor)–metal transition in expanded Hg, Se and liquid Se–Te alloys [7, 8] and semiconducting behaviour of several alloys [9], attracted wide attention.

On the other hand, high-pressure studies on crystalline solids reveal a wide variety of structural responses to increasing pressure. The compression mechanism depends on anisotropy in bonding. Many metallic elements have a dense-packed structure so that they are usually uniformly compressed. Compression of an isotropic three-dimensional network structure such as the diamond structure is also uniform. However low-dimensional structures, such as layer, chain and molecular structures, show highly anisotropic behaviour. While inter-layer (chain, molecular) distance strongly decreases with increasing pressure, the length of strong bonds within the layer (chain, molecule) is almost constant [10–12]. Pressure mainly reduces the length of weak bonds and hence reduces structural anisotropy.

Further increase of pressure often induces a structural phase transition [13]. In general, elements that have open-packed crystalline structure transform toward dense-packed structure through successive pressure-induced phase transitions: coordination number, CN, increases at the transitions. For example, Si transforms from diamond structure (CN $= 4$) to the β-tin structure (CN ~ 6), orthorhombic phase (CN ~ 6), simple hexagonal structure (CN $= 8$), orthorhombic phase (CN $= 10, 11$), hexagonal close-packed structure (CN $= 12$) and face-centred cubic structure (CN $= 12$) [14]. The electronic structure also changes under pressure and a non-metal to metal transition usually takes place. Not only covalent solids, but also some metallic elements, exhibit pressure-induced structural transitions. In exceptional cases, a decrease of the coordination number is observed in a high-pressure phase [13].

The similarity in the short-range order between the liquid and solid states, together with the rich structural changes in the solid state under pressure, promise a wide variety of structural changes in the liquid state under high pressure. The question is how the structural changes in the liquid state occur. It is natural to think that the structural response to the increasing pressure in the liquid state also depends on anisotropy in bonding. It is also expected that liquids with open-packed local structures evolve into dense-packed local structures under high pressure. But the structural changes in the liquid state have different characteristics. In the liquid state, rapid motions of atoms and the lack of long-range order allow a broad distribution of the local atomic arrangements. The broad distribution is supposed to smooth the structural change that corresponds to the pressure-induced phase transition in the solid state: a local structure similar to low-pressure structure and that similar to high-pressure structure are probably mixed in the liquid state. The smoothness, however, does not mean that the structural change in the liquid is completely monotonic. There may be pressure regions where the changes in structure and electronic properties rapidly occur.

One of the first notions on the structural change that corresponds to the pressure-induced phase transition appeared in the 1960s in connection with high-pressure melting-curve

maxima. Although the melting temperatures of most elements increase monotonically with increasing pressure, the melting temperatures of some elements such as Cs, Bi and Te have a maximum. In the region where the melting curve has a negative slope, the molar volume of the liquid is less than that of the solid. Hence the occurrence of the maximum indicates an anomalous decrease in volume in the liquid state. It was noticed that in all known cases where maxima are present, the crystalline solid also exhibits a solid–solid phase transition at some higher pressure accompanied by a large volume change. A two-species model was proposed to explain their existence [15]. In the model, the liquid was assumed to consist of two species with a transition to the denser species taking place continuously with increasing pressure. Around the melting-curve maximum, relatively rapid change of concentration of two species was predicted. However structural studies on liquids at high pressures of the gigapascal region were very limited mainly due to experimental difficulty [16]. In order to observe the structural changes directly, Tsuji *et al* [7, 17, 18] developed an x-ray diffraction method using a large-volume press and a synchrotron radiation source in the middle of the 1980s. Since then we have continued systematic study on elemental liquids such as that which will be reviewed here. So far we have been concerned with sp-bonded elements. We studied elements that may have a melting curve maximum such as Cs, Rb, Se, Te and P. Elements that have a negative melting curve slope such as Ga, Si, Ge and Bi were also studied. We have extended the study to I (iodine), which exhibits metallization and molecular dissociation in the solid state under high pressure. Besides these elements, light alkali metals, Na and K, were studied as typical simple metals.

More examples of sharp changes are reported by Brazhkin *et al* [19–25]. In the late 1980s, they started a systematic study on elemental liquids under high pressure by an electrical conductivity measurement and a thermobaric analysis, which detects a jump of sample volume [19]. They reported sharp changes of the electrical conductivity and volume changes in the liquid state at a boundary in the pressure–temperature phase diagram for several elements such as Sn [20], Sb [21], Bi [22], S [23], Se [24], Te [25] and I [26]. The term 'sharp' in their studies means that the transitions take place in pressure–temperature intervals that are rather narrow in comparison to the average values: $\Delta T \sim 50$ K at temperatures of about 1000 K, $\Delta P \sim 0.5$ GPa at pressures of several GPa. We tried to detect structural changes accompanying the reported changes.

Although no thermodynamic principles are violated by a first-order liquid–liquid transition in a single-component system, it is an extremely rare phenomenon. Thus one of the challenging problems is to give experimental evidence of such a transition [27–29]. In fact, some evidence for existence of first-order transitions in disordered materials has been found recently. Mishima *et al* [30] discovered a first-order transition between low- and high-density ices. A possibility of a first-order liquid–liquid transition was then proposed for super-cooled water [31]. Recently, we have found an abrupt structural change in liquid phosphorus [32]. Experimental results support the view that it is a first-order liquid–liquid transition between two thermodynamically stable phases.

This paper is organized as follows. In section 2, experimental methods developed for the structural studies on liquids under high pressure are briefly explained. In section 3, three topics are presented. Firstly, examples of structural changes are presented by showing similarity between a high-pressure structure of a light element and a normal-pressure structure of a heavy element in the same group of the periodic table. Secondly, variety of structural changes in several elemental liquids is illustrated through pressure dependence of the nearest-neighbour distance. Thirdly, study on the liquid–liquid transition in phosphorus is reviewed. In section 4, concluding remarks are given.

2. Experimental details

To generate high-pressure and high-temperature conditions, large-volume presses (LVPs) are usually used. The highest pressure depends on the size of the anvils. For a cubic-type multi-anvil apparatus, high pressures up to about 2, 5, 9 and 12 GPa can be generated with tungsten carbide anvils with flat squares of 10×10, 6×6, 4×4 and 3×3 mm^2, respectively. For pressure-transmitting material, a mixture of boron and epoxy resin is usually used. The sample size depends on the anvil size and it varies in diameter from 1 to 3 mm. The samples are put in a sample capsule made of boron nitride or NaCl. High temperatures up to about 1200 °C are easily reached with a graphite internal heater. Temperature is monitored by a thermocouple. Sometimes it is estimated by electric power to the heater. NaCl is usually used for an internal pressure marker. The pressure range is to extend to above 20 GPa when a double-stage type press is used. Recently Funamori and Tsuji have carried out experiments on liquid Te up to 22 GPa [33] and liquid Si up to 23 GPa [34]. Another type of LVP, the so-called Paris–Edinburgh press, that is equipped with toroid-type anvils, is also used for high-pressure x-ray diffraction [35].

In diffraction experiments using an LVP, materials that surround the sample also scatter x-rays and produce strong background x-rays. Because the x-ray diffraction pattern of a liquid sample is weak and broad, the background easily overshadows it. The use of strong, high-energy and low-divergence x-rays from synchrotron radiation sources greatly reduces this difficulty. It allows us to use a thick sample and a sharp slit system to eliminate the background. Energy dispersive x-ray (EDX) diffraction is widely used with cubic-type multi-anvil presses because one of the x-ray sources, a bending magnet, produces white (polychromatic) x-rays and because the diffraction pattern can be taken at a fixed angle. The observed coherent x-ray intensity at 2θ, $I(E, 2\theta)$, may be expressed as

$$I(E, 2\theta) = A(2\theta) I_0(E) f^2(Q) S(Q) I_{det}(E) \Sigma \exp(-\mu_i \rho_i t_i)$$
$$Q = 4\pi \sin\theta/\lambda = 4\pi \sin\theta \times 10^{-7} \times eE/hc = 4\pi E \sin\theta/12.398$$

where E is the energy of the x-ray in keV, Q is the wavenumber in Å^{-1} and $A(2\theta)$ is a constant that depends on ring current, data acquisition time and sample volume. $I_0(E)$ is the energy distribution of the incident x-ray, $f(Q)$ is the atomic form factor, $S(Q)$ is the structure factor, $I_{det}(E)$ is the energy dependence of the sensitivity of the detector, μ_i, ρ_i and t_i are respectively the x-ray mass absorption coefficient, density and thickness of material i in the x-ray path, λ is the x-ray wavelength, e is the elemental electric charge, h is the Planck constant and c is the speed of light. To obtain $S(Q)$, precise determinations of these terms are needed. However, it is difficult to determine the energy dependence of each term from first principles. For example, ρ_i and t_i change under compression. To solve this problem, Tsuji *et al* [18] proposed an empirical method to estimate the total correction term. In this analysis, $I(E, \theta)$ measured at several 2θ angles, typically about 10 angles from 3° to 20°, are used. They introduced an energy-dependent function $C(E)$ and assumed that $I(E, \theta)$ is expressed as

$$I(E, 2\theta) = A(2\theta) f^2(Q) S(Q) C(E).$$

In this assumption $C(E)$ is independent of 2θ. Since $S(Q)$ values for different 2θ should be the same, $C(E)$ can be constructed by a iterative procedure minimizing the difference between the $S(Q)$ values calculated at several 2θ values. Later, Funakoshi [36] developed a computer program for the construction of $C(E)$ using a Monte Carlo method. The program is used to analyse the data of liquid P. Experimental data shown here were measured using cubic-type multi-anvil presses, MAX90 at the BL14 beamline at the Photon Factory, MAX80 at the ARNE5 beamline at the Tristan accumulation ring and SMAP180 at the BL14B1 beamline at SPring-8.

The angle-dispersive x-ray (ADX) diffraction method has an advantage in reliable diffraction data because fewer corrections are needed to obtain $S(Q)$. With a single-collimator system and a bending magnet source, however, the method is not practical because very long data acquisition time is needed. Development of a multi-channel collimator system [37] together with a use of strong x-ray beam from insertion devices in third-generation synchrotron radiation sources greatly shortens the data acquisition time.

XAFS (x-ray absorption fine structure) is a complementary method for study on local structure. Since information from high-pressure x-ray diffraction experiments is limited as compared with normal-pressure experiments, additional information is desirable. The XAFS is very sensitive to the local atomic arrangement. In addition, it has chemical selectivity. By combining LVP and synchrotron radiation, we have successfully measured x-ray absorption spectra of liquid Se up to 8 GPa [38].

Density is one of the most important parameters to discuss structural change. However there has been no efficient method for its measurement under high pressure and temperature. A problem in the x-ray absorption method lies in the uncertainty of sample thickness under high pressure. To solve the problem, we put a sapphire ball in the sample capsule as a calibrant of the sample thickness and measured x-ray absorption as a function of sample position [39]. Alternatively, we use a sapphire ring as a sample container [40]. For a cylindrical sample in the ring, the absorption by the sample along an axis, x, perpendicular to the cylindrical axis is expressed by the following formula:

$$I/I_0 = C \int_{beam} \exp(-\mu\rho l(x))\,\mathrm{d}x, \qquad l(x) = (r^2 - (x - x_0)^2)^{1/2},$$

where C is a constant, μ, the mass absorption coefficient of the sample, ρ, the density of the sample, $l(x)$, the length of the path in the sample, r, the diameter of the sample, and x_0, the centre of the sample. The integration was done over the beam size. From a curve fit of the absorption profile, the density can be obtained. Using intense, high-energy and low-divergence x-rays from synchrotron radiation sources, we can measure the absorption profile as a function of sample position precisely, even though the sample is as small as 0.5 mm in diameter [40].

3. Results and discussion

3.1. Structural similarity in the same group

From x-ray diffraction experiments on elemental liquids under high pressure, we obtained data that indicate the close relationship between the solid and liquid structures under high pressure. Tsuji *et al* have measured x-ray diffraction of liquid Se and found that the structure factor, $S(Q)$, for liquid Se at 8.4 GPa was very similar to that for liquid Te, at atmospheric pressure [7, 17]. This resemblance between the high-pressure structure of the light element (Se) and the normal-pressure structure of the heavy element (Te) in the same group is interesting because a similar relation has already been recognized in the crystalline state. Se and Te, group VI elements, have the same crystalline structure, that consists of chain molecules. The structural anisotropy, a ratio of the length of the weak inter-chain bond over that of the strong intra-chain bond, is larger in Se. Pressure reduces the structural anisotropy in crystalline Se and changes the structure toward a Te-like structure. The similarity in $S(Q)$ indicates that pressure also changes the structure of liquid Se to a liquid-Te-like structure.

Since then, more examples have been found. Figure 1 shows the structure factor, $S(Q)$, for another group VI element, S, at 7.6 GPa and 750 °C [41] together with that for Se at

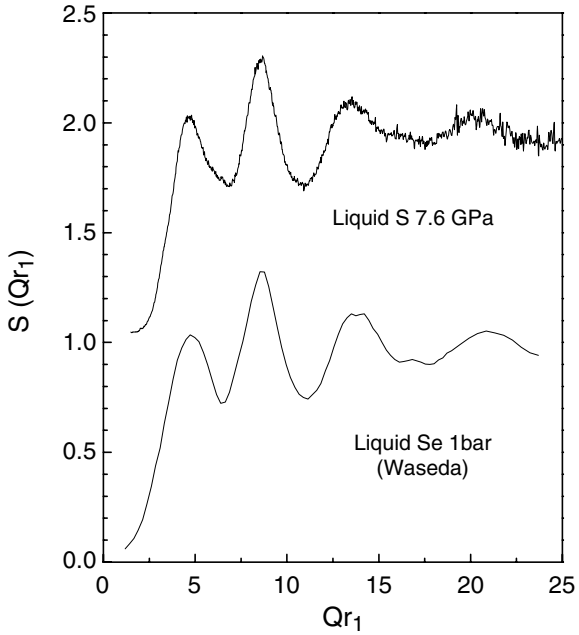

Figure 1. Structure factors, $S(Q)$, for liquid S at 7.6 GPa and that of liquid Se at atmospheric pressure [1] as functions of Q multiplied by the nearest-neighbour distance, r_1, of each liquid.

atmospheric pressure reported by Waseda [2]. To compensate for the effect of different atomic sizes of the two elements, the structure factors are plotted as a function of Qr_1, where r_1 is the first-nearest-neighbour distance, that is evaluated from the position of the first peak in the pair correlation function $g(r)$. A close resemblance between the two curves indicates that the local structure of liquid S at high pressure is close to that of liquid Se at atmospheric pressure. Liquid Se consists of long chain molecules. While liquid S just above the melting point at atmospheric pressure is a molecular liquid that consists of S_8 ring molecules, it undergoes a so-called 'λ-transition' upon heating and the main constituents are long chains above 159 °C [6]. Closer packing of chain molecules by compression of liquid S makes the two structures alike. A polymerization was also reported in the crystalline state under pressure [42]: S transforms from a crystal composed of S_8 molecules to a crystal with chain molecules under high pressure, although the structure of the high-pressure phase is not exactly the same as that of Se.

Figure 2 shows $S(Qr_1)$ for liquid P at 4.6 GPa and 1200 °C [43] together with that for liquid As at 0.47 MPa and 825 °C reported by Bellissent *et al* [44]. The similarity between the two curves indicates that the local structure of molten black P under pressure is similar to that of liquid As at atmospheric pressure. This change again corresponds to the transition in the crystalline state. The most stable form of P at atmospheric pressure, black P, transforms to the arsenic (As) structure around 3 GPa near the melting temperature.

Similarities in $S(Q)$ are also reported in group IV elements. It is known that crystalline Si transforms from the diamond structure to the beta-Sn structure near 12 GPa. The structure factors of liquid Si at 4 and 8 GPa are similar to that of liquid Ge at atmospheric pressure and those at 14 and 23 GPa are similar to that of liquid Sn [34]. These similarities confirm that there is some parallelism between the structural changes in the liquid state and those in the solid state in group IV, V and VI elements.

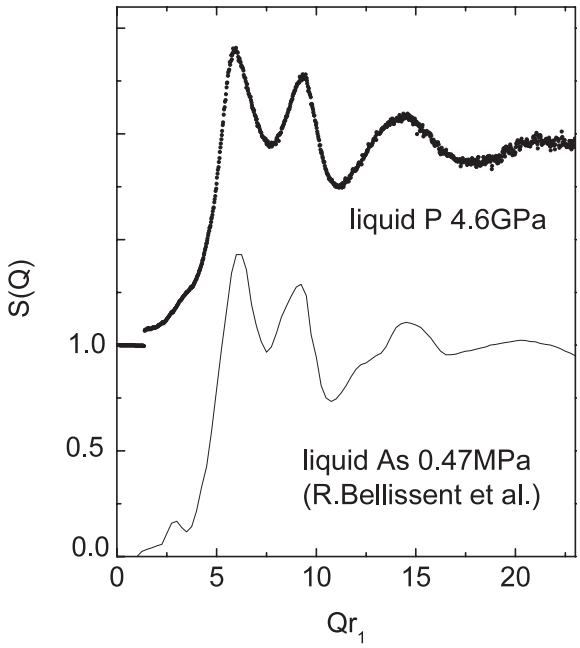

Figure 2. Structure factors, $S(Q)$, for liquid P at 7.6 GPa and that of liquid As at atmospheric pressure [43] as functions of Q multiplied by the nearest-neighbour distance, r_1, of each liquid.

3.2. Pressure dependence of nearest-neighbour distance

The relations between liquid and solid structures presented in the previous section suggest that each element shows distinct structural changes in the liquid state. To illustrate the point in detail, we plot $r_1/r_1(0)$, the position of the first peak in the pair distribution function $g(r)$, r_1, normalized by that at atmospheric pressure, $r_1(0)$, as a function of $(V/V_0)^{1/3}$ in figure 3 for alkali metals, in figure 4 for Ga, Si and Ge and in figure 5 for Bi, Se, Te and I. The pair distribution functions were obtained from energy-dispersive x-ray diffraction measurements carried out just above the melting temperature under high pressure. The position of the first peak corresponds to the first-nearest-neighbour distance. Here V is the molar volume and V_0 is the molar volume at atmospheric pressure. There are almost no data on the volume of the liquids under high pressure and high temperature so that the volumes are estimated from those of crystalline solids under high pressures and high temperatures, and the volume jump at the melting. The volume jump is estimated as follows. From the Clausius–Clapeyron equation, the slope of the melting curve is proportional to the volume jump on melting and it is inversely proportional to the change of the entropy on melting. Hence the volume jump can be roughly estimated from the reported value at atmospheric pressure and the melting curve, assuming that the entropy change does not undergo a large change with pressure.

Alkali elements have only one s electron as a valence electron and they are regarded as 'simple' metals. The structure of liquid alkali metals at atmospheric pressure is well described by a simple hard-sphere-like model [2]. High-pressure x-ray diffraction measurements on liquid alkali metals were carried out up to 5.1 GPa for Na, 6.1 GPa for Rb and 4.3 GPa for Cs. Figure 1 shows $r_1/r_1(0)$ for alkali metals, Na [45], K [45–47], Rb [45, 46, 48] and Cs [49]. If the liquid is compressed uniformly, $r_1/r_1(0)$ follows a relation of $r_1/r_1(0) = (V/V_0)^{1/3}$. The relation is indicated by a solid line in figure 3. The experimental data agree with the relation:

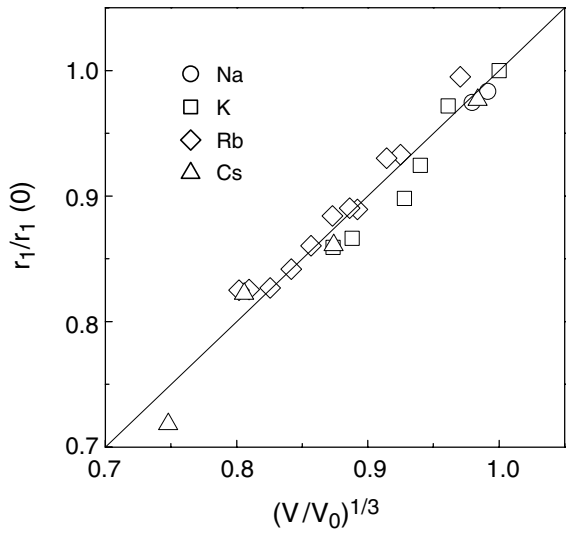

Figure 3. Volume dependence of nearest-neighbour distance, r_1, for liquid Na, K, Rb and Cs. Volume, V, and r_1 are normalized by values at atmospheric pressure, V_0 and $r_1(0)$, respectively, and $(r_1/r_1(0))$ is plotted as a function of $(V/V_0)^{1/3}$.

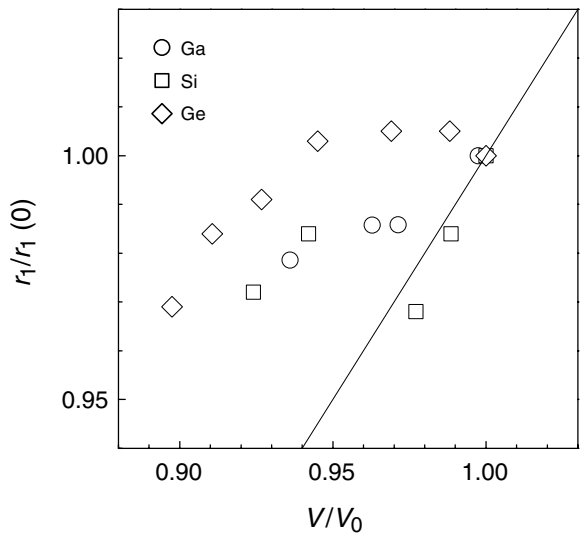

Figure 4. Volume dependence of nearest-neighbour distance, r_1, for liquid Ga, Si and Ge.

liquid alkali metals are almost uniformly compressed. The coordination number is already high at atmospheric pressure, so that a drastic change in the local structure is not realized under high pressure. Closer analysis of r_1, coordination numbers and the position of the first peak in $S(Q)$, however, showed that there are slight deviations from the uniform-compression model in Rb and Cs at $(V/V_0)^{1/3} < 0.85$. The most notable deviation is observed in the position of the first peak in $S(Q)$, Q_1: it becomes lower than that expected from the uniform-compression model. The deviation may suggest a structural change to a denser structure because it implies longer

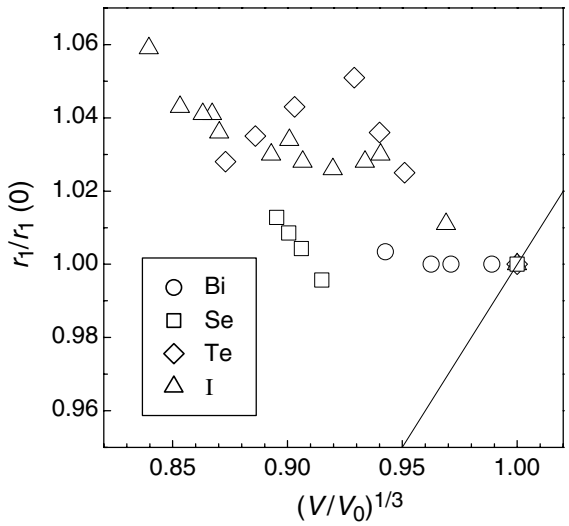

Figure 5. Volume dependence of nearest-neighbour distance, r_1, for liquid Bi, Se, Te and I.

atomic distances and hence larger coordination number. This deviation may be obscured in $g(r)$ by experimental errors. The deviations are considered to be due to an s–d electronic transition in Rb and Cs. The s–d transition is believed to play an important role in a unique pressure-induced phase transition sequence of heavy alkali metals [13, 50]. At atmospheric pressure, Rb and Cs have body-centred cubic structure. They transform to face-centred structure and then transform to complex structures. A first-principles molecular-dynamics simulation study on liquid Rb under high pressure confirms the change to denser structure [51]. However another theoretical study on liquid Rb under pressure showed no deviation in the pressure dependence of structure factor up to 6.1 GPa, the highest pressure in our experiments [52].

Elements that have p electrons as valence electrons tend to form covalent bonds. Therefore they usually have open-packed structures in the solid state. Figure 4 shows the volume dependence of the first peak position in $g(r)$, r_1, for liquid Ga [53, 54], Si [34] and Ge [55]. The $g(r)$ values were obtained by energy-dispersive x-ray diffraction measurements up to 6.1 GPa for Ga, 23 GPa for Si and 25 GPa for Ge. The solid line indicates the relation $r_1/r_1(0) = (V/V_0)^{1/3}$. The volume dependence clearly shows deviations from the relation: these liquids are not uniformly compressed. Ga is a group III element and it has one p electron. It has distorted hexagonal close-packed structure in the crystalline state at atmospheric pressure. The structure of liquid Ga is not simple: the structure factor has a distinct shoulder on the large-Q side of the first peak. The existence of the shoulder indicates that the structure of the liquid is not fully described by a simple hard-sphere-like model. The deviation from the simple hard-sphere-like model is ascribed to an oscillatory part of the inter-atomic potential [3] or partial-covalency effects [2]. The nearest atomic distance for Ga in the liquid state continuously decreases with volume contraction but the decrease is smaller than that expected from the uniform-compression model. The compression of Ga is accompanied by a continuous increase of coordination number [53]. The local structure evolves toward a less anisotropic one under pressure.

Although Si and Ge, group IV elements, are typical semiconductors in the crystalline state with the diamond structure formed by sp^3 hybridized orbital, they are metallic in the liquid state. The coordination number increases from four to six upon melting. Since the coordination

number is much lower than that of simple metallic liquids, it is supposed that covalent components in bonding still exist in the liquid state. The volume dependence of r_1 for liquid Si is complicated [33]: it decreases initially almost obeying the relation $r_1/r_1(0) = (V/V_0)^{1/3}$ and then increases suddenly between 8 and 14 GPa. After that r_1 decreases again. The sudden increase of r_1 is accompanied by a change in the shapes of $S(Q)$ and a significant increase of the coordination number. This behaviour suggests a structural transformation to a denser structure between 8 and 14 GPa: there are two regions in the liquid state. The almost uniform compression in each region is attributable to three-dimensional-network character in liquid Si. Liquid Ge also shows complicated behaviour. The nearest neighbour distance is almost constant up to $V/V_0 = 0.94$ and then decreases almost uniformly.

Group V, VI and VII elements tend to form low-dimensional structures such as layers, chains and molecules. The structures can be understood as a Peierls distortion of a sixfold coordinated structure. The coordination numbers follow the $8 - N$ rule (N is the number of s and p valence electrons) and formation of strong bonds between atoms distorts the prototype simple cubic structure. Figure 5 shows the volume dependence of r_1 for Bi [56], Se [57], Te [33] and I [58]. Energy-dispersive x-ray diffraction measurements were carried out up to 4.7 GPa for Bi, 4.9 GPa for Se, 22 GPa for Te and 10.6 GPa for I. The solid line indicates the relation $r_1/r_1(0) = (V/V_0)^{1/3}$. There are marked deviations from the uniform-compression model. Bi, a group V element, has layer structure in the crystalline state. The structural anisotropy is rather small: each atom has three intra-layer nearest atoms at 3.072 Å and three inter-layer second-nearest atoms at 3.529 Å. The liquid structure deviates from the simple hard-sphere-like structure, though the atoms are no longer threefold coordinated. The nearest-neighbour distance is almost constant under pressure. The compression of Bi is due to an increase of coordination number [56].

Group VI elements tend to form twofold covalent bonds. Crystalline Se and Te are composed of infinite chain molecules. The nearest-neighbour distance for liquid Se is almost constant up to $(V/V_0)^{1/3} = 0.92$ and then increases in spite of compression. That for liquid Te initially increases and then decreases. These anomalous increases of nearest neighbour distance are attributed to a modification of the covalent bonds. In liquid Se, the chain molecules are largely preserved and liquid Se is a typical liquid semiconductor. The initial compression is due to reduction of inter-chain distance and the covalent bond length is unchanged. When the chains are packed more closely, overlap of the non-bonding orbital and anti-bonding orbital interfere with intra-chain covalent bonds and weakening and/or breaking take place. During this process, the nearest-neighbour distance elongates. The modification of the covalent bonds is also confirmed by high-pressure EXAFS studies [38]. The EXAFS oscillation originates from the fact that the nearest-neighbour correlation in the liquid state is almost the same as that in the solid state at low pressure but it significantly decreases in the metallic region. This structural change is accompanied by a change of electronic structure: the observed change of the bond length by x-ray diffraction coincides with the reported semiconductor-to-metal transition, which has a liquid–liquid–solid triple point at $P = 3.6 \pm 0.5$ GPa and $T = 627\,^{\circ}$C. Furthermore, this metallization is supported by the similarity between $S(Q)$ of liquid Se under high pressure and that of liquid Te at atmospheric pressure because liquid Te is already metallic at atmospheric pressure. A semiconductor-to-metal transition also occurs by an increase of Te concentration in liquid Se–Te alloys at atmospheric pressure [7]. The pressure and the chemical substitution have similar effects on structure and electronic properties of liquid Se [59]. A volume jump is reported at the semiconductor-to-metal transition in liquid Se [24]. This change is probably an equivalent of an anomalous concentration dependence and temperature dependence of density in Se–Te alloys. Direct measurements on the density of liquid Se under high pressure are currently under way.

Liquid Te is supposed to consist of entangled short chains. The initial increase of atomic distance in liquid Te indicates that the weakening of the twofold covalent bonds proceeds with increasing pressure. The nearest-neighbour distance of liquid Te starts to decrease below $(V/V_0) = 0.92$. The maximum of r_1 is observed at 6 GPa. Around the pressure, at 5 GPa, a sharp change of electrical conductivity was reported [25]. In our previous x-ray diffraction and density measurements, some anomalies were suggested in this region [39, 60]. However, the existence of a sharp structural change is still controversial because observed anomalies are comparable to the experimental errors. The change of the volume dependence of r_1 suggests a different mechanism of compression above 6 GPa. The decrease of r_1 is smaller than that expected from the uniform-compression model. A mild structural change with an increase of the coordination number progresses in this pressure range. The structure of liquid Te at 22 GPa, the highest pressure in the study, approaches a simple metallic liquid, although there is a deviation in the structure factor.

The halogens are all diatomic molecules. Both crystalline and liquid phases of iodine are composed of I_2 molecules. No evidence for dissociation of molecules was observed in the diffraction study up to 10.6 GPa: the diatomic molecular structure is preserved at this pressure [58]. As shown in figure 5, r_1, which corresponds to the intra-molecular bond length, continuously increases in spite of compression. This result is consistent with a previous EXAFS study [61]. On the other hand, the inter-molecular distance, which is determined by the position of the second peak in $g(r)$, decreases with increasing pressure [58]. Therefore the elongation of covalent bonds is attributed to an interference of the inter-molecular interaction strengthened by the decrease of inter-molecular distance. The elongation of the covalent bonds is much larger than that of crystalline I_2 at the same pressure. The larger elongation may be due to frequent close approaches of molecules, which are induced by rapid motions of molecules and lack of long-range order in the liquid state. Around 4 GPa, two boundaries for a sharp increase of electrical conductivity in the liquid I were reported [26]. No evidence for molecular dissociation indicates that metallization occurs in the molecular phase as in the case of the solid state. In the solid state, a molecular phase transforms to a high-pressure phase in which the intra-molecular atomic distance and the inter-molecular atomic distance become the same: a molecular dissociation occurs at the transition at 21 GPa. On the other hand, metallization takes place around 15 GPa, in the molecular phase. It is induced by an overlap of valence and conduction bands. The lower transition pressure in the liquid state is consistent with the rapid increase of intra-molecular bond length.

The difference in volume dependence of the first-nearest-neighbour distance for these elements clearly demonstrates that the compression mechanism depends on anisotropy in bonding even in the liquid state. Uniform compression is observed in simple metallic liquids (alkali metals). Almost uniform compression is observed in liquid Si, which has three-dimensional-network character. Various degrees of deviation of r_1 from the uniform-compression model are observed in not-simple liquid metals. Compression of the low-dimensional structures is mainly due to closer packing of the structural units. The closer packing sometimes induces elongation of covalent bonds (Se, Te, I). The modification of covalent bonds is related to metallization. This behaviour can be understood in the same framework that describes structural trends of the elements [2–5, 62, 63]. Hafner *et al* showed that the trends arise from a characteristic variation of the real-space inter-atomic potential. The complex structures of the light polyvalent liquid metals arise from the interplay of two characteristic distances: the effective diameter of the hard repulsive core and the Friedel wavelength of the oscillatory part of the potentials. The volume dependence of the two distances is different so that the repulsive core moves over the attractive wiggle under pressure and the change of the potential stabilizes a more close-packed structure. An alternative view

was presented by Gaspard *et al* [62, 63]. They show that the structures of covalent elements can be explained by a Peierls instability. A moment calculation shows periodicity is not a necessary condition for getting the Peierls distortion so that the model can be applied to not only crystal structures but also amorphous and liquid structures. At small volumes, the core repulsion prevents the system from being distorted. Therefore a more close-packed structure is stabilized under high pressure.

The different volume dependence of nearest-neighbour distances in the different pressure range observed in liquid Si, Se and Te suggests that the liquid phase can be divided into various regions. However, diffraction studies on the elements presented in this section provide no direct evidence for a first-order liquid–liquid transition. The only exception is the abrupt structural change in liquid phosphorus, which will be reviewed in the next section.

3.3. Liquid–liquid transition in phosphorus

Phosphorus is a group V element. It has many allotropes in the solid state at atmospheric pressure and room temperature [4, 64]. White P is a molecular solid that consists of P_4 tetrahedral molecules. Red P is usually amorphous. It has a three-dimensional-network structure. Black P, the most stable structure, has a puckered layer structure. In spite of the wide variety of structure, the P atom is invariably threefold coordinated. White phosphorus melts at 44 °C and P_4 molecules are preserved in molten white P. Further heating transforms molten white P to red P around 200–400 °C. Black P and red P melt around 600 °C. Our x-ray diffraction study on molten black phosphorus under high pressure revealed liquid P has two distinct structures, which are supposed to be a molecular liquid and a polymeric liquid [32]. Figure 6 shows $S(Q)$ of liquid P together with that of red P at various pressures [43]. Because the melting temperature of black phosphorus is close to that of NaCl at low pressures, the pressures below 2 GPa were determined by a diffraction line of boron nitride in the sample assembly using an equation of state (EOS) reported by Zhao *et al* [65]. The pressures calculated by using another EOS of boron nitride reported by Le Godec *et al* [66] are indicated in parentheses. Pressures above 2 GPa were determined by a NaCl pressure marker. The error in the pressure determination is about ±0.3 GPa. The error in the temperature is about ±50 °C. It was large because a thermocouple broke under high temperature and the temperature was then estimated by the heater power. Below 1 GPa, $S(Q)$ of liquid phosphorus has a sharp first peak around 1.36 Å^{-1}. Above 1 GPa, the sharp first peak almost disappears and a new peak appears around 2.4 Å^{-1}. This large and sharp change of $S(Q)$ in the liquid state indicates that there are two distinct liquid forms. Here we call them the low-pressure liquid and the high-pressure liquid. The $S(Q)$ of the high-pressure form is similar to that of red P, the disordered (amorphous) solid form of P, though the first sharp diffraction peak is very small and the peaks are broadened in the liquid state. As mentioned in section 3.1, the $S(Q)$ at 4.6 GPa is very close to that of liquid As near atmospheric pressure. These similarities suggest that the high-pressure liquid is a polymeric liquid similar to that of liquid As. On the other hand, the $S(Q)$ of the low-pressure form resembles that of molten white P [67]. The $S(Q)$ of molten liquid P and low-pressure liquid are characterized by a strong first peak, fine structures between 2 and 4 Å^{-1} and relatively simple oscillation in the high-Q region. It is highly likely that the low-pressure liquid is the molecular liquid comprised of P_4 molecules. A reverse Monte Carlo analysis agrees with this assignment [68].

Figure 7 shows the radial distribution function (RDF) of red P and molten black P at various pressures and temperatures [43]. The first peak corresponds to covalent bonds. The most notable difference between the low- and high-pressure liquids is the disappearance of the second peak of the RDF in the low-pressure liquid. The feature of the RDF for the low-pressure

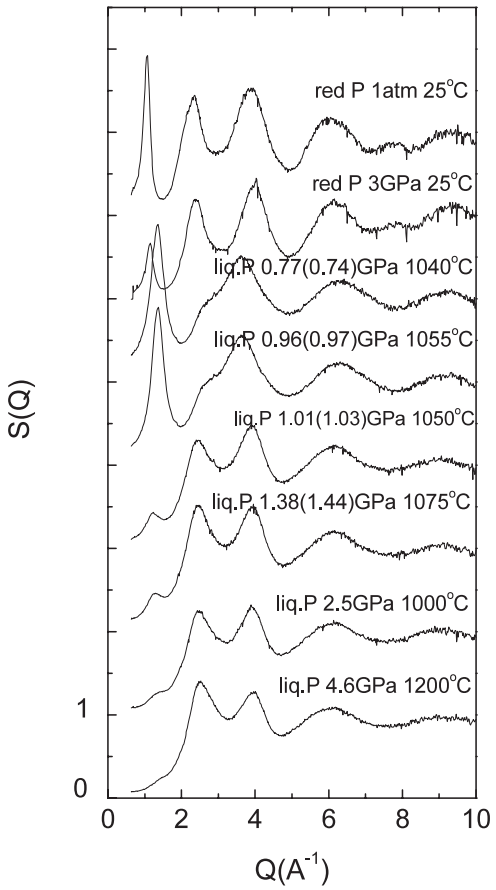

Figure 6. Structure factors, $S(Q)$, for red amorphous P and liquid P at various pressures and temperatures.

liquid supports a picture in which it is comprised of P_4 molecules, without strong bonds between them. In the high-pressure liquid, a distinct second peak appears between 3 and 4 Å. The appearance is consistent with a high-pressure liquid with a network structure, where the central and the second-nearest-neighbour atoms are connected by two covalent bonds to the first-nearest-neighbour atom. The position of the second peak coincides with the second-nearest-neighbour distance in black P. The second-nearest-neighbour distance within an extended layer structure in black P is 3.31 Å. A part of the second peak may be attributed to non-bonding atoms as in the case of the crystalline layer structures: the shortest inter-layer distance in black P is 3.59 Å. The second peak of the high-pressure liquid is broader than that of red P. It becomes broad with increasing pressure and the first and the second peaks gradually overlap each other. The maximum of the first peak shifts to larger r values from 2.29 Å at 1.01 GPa to 2.36 Å at 4.6 GPa. These values are larger than the covalent bond length in black P, which appear at 2.22 and 2.24 Å at atmospheric pressure. They are also larger than the positions of the maximum of the first peak for red P, 2.25 Å at 0 GPa and 2.22 Å at 3 GPa. The longer nearest-neighbour distance and the broadening of the second peak suggest that the network structure of the high-pressure liquid is not as rigid as its solid forms.

The low- and high-pressure liquids are obtained by melting black phosphorus below and above 1 GPa, respectively. In addition, the high-pressure liquid is obtained from the

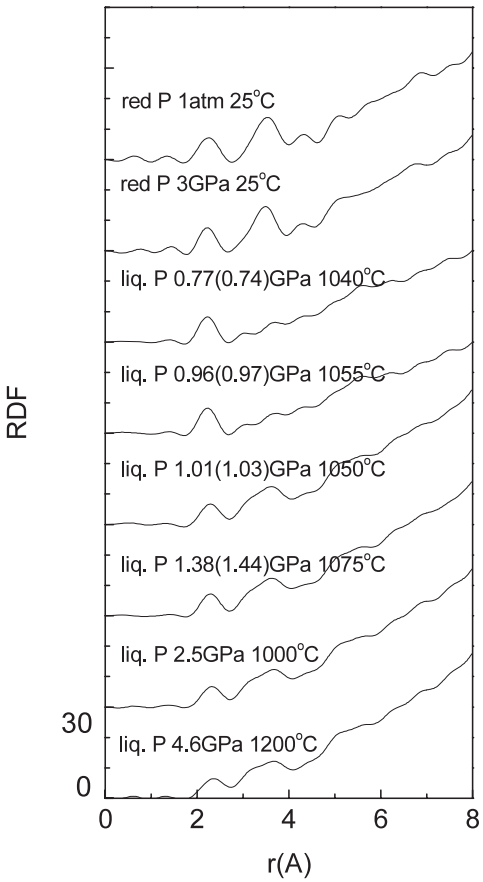

Figure 7. Radial distribution functions, RDF, for red amorphous P and liquid P at various pressures and temperatures.

low-pressure liquid, and *vice versa*, by a change in pressure [32]. The transformation is reversible and occurs within a pressure range <0.1 GPa and after a time interval of a few minutes. During the transformation, the observed x-ray diffraction patterns were reproduced by a weighted average of those of low- and high-pressure liquid: the two liquids coexist during the transformation. There is no intermediate state detectable by the x-ray diffraction measurements. This fact supports the view that the transformation is a first-order liquid–liquid transition.

If the transformation is first order, densities of low-and high-pressure liquids are different. A large difference is expected because the densities of white P, red P and black P at atmospheric pressure and room temperature are very different: they are 1.82, 2.2–2.34 and 2.69 g cm^{-3}, respectively. In addition, the reported density of liquid P is 1.69 g cm^{-3} at 100 °C and 0.96 g cm^{-3} at 680 °C [64]. According to the Clausius–Clapeyron relation, the density change upon melting is proportional to the slope of the melting curve. Therefore, we measured the melting temperature of black P as a function of pressure by the *in situ* x-ray diffraction method to confirm the density change [69]. We used the EOS formulated by Zhao *et al* in previous reports [32, 43, 69]. After the publication of these, we noticed that there are large discrepancies among the reported EOSs for boron nitride. There are at least three determinations of the EOS

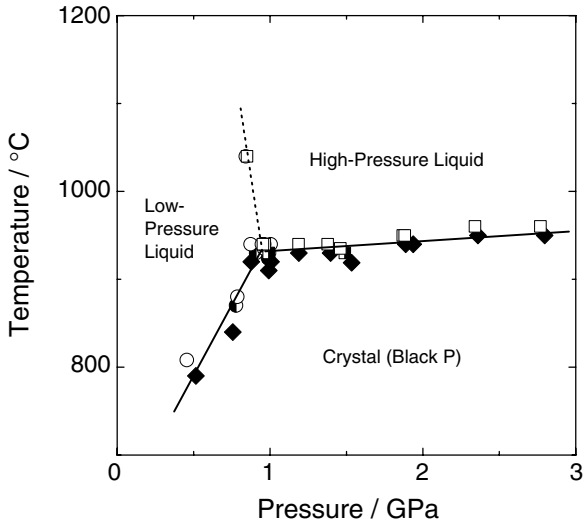

Figure 8. Pressure–temperature phase diagram of black P. Closed diamonds (♦), open circles (○) and open squares (□) indicate points where crystalline black P, the low-pressure liquid and the high-pressure liquid were observed, respectively.

by high-pressure, high-temperature x-ray diffraction methods [65, 66, 70]. Although the three groups used a similar experimental technique, the results were very different. The calculated pressures differ by more than 40%. The EOS by Zhao *et al* usually gives the lowest pressure. In a few experimental runs, we used both NaCl and boron nitride pressure markers in the same assembly. A relatively good agreement was found between the pressures determined by the NaCl marker and those determined by the boron nitride marker using the EOS by Le Godec *et al* in the low-temperature region below the melting temperature. Therefore we adopt the EOS by Le Godec *et al* here. The error in the absolute value of pressure is about ± 0.2 GPa. The temperatures were monitored by a thermocouple. The error in temperature is about $\pm 20\,^{\circ}$C. Figure 8 shows the results. It is found that the melting temperature increases rapidly with increasing pressure up to 1.0 GPa. In this region black P melts into the low-pressure liquid. Above this pressure, the melting temperature increases slightly. In this region, black P melts into the high-pressure liquid. The discontinuous change of the slope of the melting curve at the transition pressure between low- and high-pressure liquid indicates that the two liquids have different densities. The almost flat melting curve below the high-pressure liquid implies that the density change upon melting is small: the density of the high-pressure liquid is almost the same as that of black phosphorus.

A previous study based on x-ray diffraction measurements on the melting curve of black phosphorus showed the existence of a melting curve maximum. However the curve was determined by a few experimental points in the previous study so that the result is not precise [71]. Another study showed a gradual increase of melting temperature up to 1.7 GPa. In this study, the pressure was not measured by an *in situ* method: we suppose that there were large errors in the pressure determination [72]. There is a possibility that we underestimate the pressure due to the errors in the EOS of boron nitride. It was shown that the EOS of boron nitride was very sensitive to the defects in boron nitride [66]. Further refinement of the pressure determination from the comparison between the NaCl and boron nitride pressure markers is currently under way. Results will be reported elsewhere.

For the low-pressure liquid, a model liquid of uncorrelated P_4 molecules roughly reproduces $S(Q)$ [43]. The fine structure between 2 and 4 $Å^{-1}$ arises from correlation between the molecules. It is pronounced in molten white P, whereas it is small in the low-pressure liquid. Correlations between molecules are small presumably due to rapid molecular motions at high temperature. The model calculation gives densities of 1.5 g cm^{-3} at 0.77 GPa and 1.6 g cm^{-3} at 0.96 GPa. The estimation of error in this analysis is difficult and it may be more than 10%. Even so, it is certain that the density of the low-pressure liquid is much lower than that of the high-pressure liquid, which has density similar to that of black phosphorus. This is further evidence for the first-order transition. Analysis of direct measurements of the densities of low- and high-pressure liquids by the x-ray absorption method is currently under way and the results will be reported elsewhere.

First-principles MD simulations realized the structural transition of liquid phosphorus. Before our high-pressure studies, Hohl and Jones [73] reported the first simulation study of the polymerization transition of liquid phosphorus. They observed a polymerization of P_4 molecules by heating the molecular liquid in a constant-volume simulation cell. After our report [32], the pressure-induced transition was realized in the molecular dynamics simulations. Morishita [74] used the constant-pressure method. The molecular phase was produced in the simulation box and the polymerization was observed by a pressure change from 0.7 to 2.5 GPa. The same transition is also realized by heating. Senda *et al* [75] used a constant-volume method and obtained both the molecular liquid phase and the polymeric liquid phase at different densities. The P_4 molecules were stable at the low density of 1.7 g cm^{-3} while they polymerized at the high density of 2.8 g cm^{-3}. The simulation results reproduced the $S(Q)$ of low- and high-pressure liquid obtained in our experiment. In their simulations, the P–P bonds are sometimes broken and rearranged to form bonds with the other P ions in the polymeric liquid, whereas the P_4 molecules never broke in the molecular liquid. Senda *et al* [75] reported that the transition is accompanied by a nonmetal–metal transition. This is consistent with a report of metallization of liquid P under high pressure [19]. Morishita [76] studied the structure of the polymeric liquid at higher pressures by molecular dynamics simulations. A gradual transition from a threefold coordinated structure to a sixfold coordinated structure was reported. The transformation is interpreted by a suppression of the Peierls distortion. It is consistent with our results of gradual structural changes in the high-pressure liquid.

The experimental evidence and the results of MD simulations support a view that it is a first-order liquid–liquid transition. In spite of the progress, it is still unclear why phosphorus exhibits such drastic structural change. One of the key points is the stability of the molecular phase over the polymeric phase. It is very unusual that a crystal with a network structure melts into a molecular liquid. It is supposed that the rigid network structure composed of three- or fourfold coordinated atoms may be unfavourable in the liquid state due to its low entropy. Sufficiently high temperature and/or high pressure may be necessary to realize the high mobility of atoms in the three- or fourfold coordinated structures. Another point is the immiscibility of low- and high-pressure liquids. A chain reaction model was proposed to understand the polymerization transition of liquid P [73]. As the temperature and density are increased, P_4 molecules undergo more collisions with other tetrahedra. Above a threshold thermal energy, locally stable defects with fourfold coordination link the P_4 molecules. The resulting objects decay by breaking a single bond in the tetrahedra to form 'roof' structures. This is accompanied by the increase in the number of twofold coordinated atoms. The twofold-coordinated atom has a dangling bond so that it is very reactive: the increased number of twofold coordinated atoms means that reactions between P_4 units are more probable. When the twofold defect attacks an intact P_4 molecule and forms a bond, a new twofold defect is created in the attached P_4 unit. In other words, the defect moves to the end of the aggregate. It then attacks another P_4 unit. By

this defect-mediated chain reaction, the transformation spreads through the sample [73]. Hohl and Jones also proposed that this reaction can be initiated not only by those atoms that have twofold coordination but also by their neighbouring atoms, and the species attacked include all twofold and threefold coordinated atoms. The result is a wide spectrum of branched growing species [73]. The high reactivity of the aggregates, i.e. polymeric liquid, may destabilize a microscopic mixture of the molecular and polymeric liquids. Once it is formed, it dissociates other P_4 molecules and incorporates with them very quickly. Then the large difference in density between the two phases may suppress the reverse process. This may be a reason why we do not see any intermediate state by the x-ray diffraction method.

4. Concluding remarks

Systematic studies of the structure of elemental liquids under high pressure reveal that there is some parallelism between the structural evolution in the solid and liquid states. The structural response to increasing pressure depends on the local anisotropy in bonding even in the liquid state. The trends can be understood within the same framework that describes the crystal and liquid structures of the elements. The structural changes in the liquid state are usually continuous but they are not completely monotonic. The sharp structural change in liquid P is very special. Experimental evidence and results of simulations support a view that it is a first-order liquid–liquid transition. In spite of some progress, it is still unclear why liquid P exhibits such a transition. Because the transition is accessible by several experimental techniques, we hope that further studies will answer the questions. Finally, we point out that high-pressure and high-temperature studies have recently been extended to a liquid transition metal [77], liquid alloys [78–80] and oxide glasses [81]. The progress in high-pressure studies helps our understanding of the structure and properties of disordered materials. It may give other examples of the sharp structural transition in the disordered state.

Acknowledgments

We thank Drs O Shimomura, W Utsumi, M Yamakata, K Funakoshi, T Mizutani, K Nakano, T Kikegawa, N Funamori, T Hattori, K Yoaita, N Hamaya and many other collaborators in our study. The experiments were carried out in the Photon Factory and SPring-8. We thank many staff members in the facilities for their support.

References

[1] Brazhkin V V, Buldyrev S V, Ryzhov V N and Stanley H E 2002 *New Kinds of Phase Transformations: Transformations in Disordered Substances* (New York: Kluwer)
[2] Waseda Y 1980 *The Structure of Non-Crystalline Materials* (New York: McGraw-Hill)
[3] Hafner J and Kahl G 1984 *J. Phys. F: Met. Phys.* **14** 2259
Hafner J and Jank W 1992 *Phys. Rev.* B **45** 2739
[4] Donohue J 1974 *The Structure of the Elements* (New York: Wiley)
[5] Hafner J and Heine V 1983 *J. Phys. F: Met. Phys.* **13** 2479
[6] Mayer B 1975 *Chem. Rev.* **76** 367
Bellisent R, Descotes L, Boue F and Pfeuty P 1990 *Phys. Rev. Lett.* **41** 2135
Winter R, Szornel C, Pilgrim W-C, Howells W S, Egelstaff P A and Bodensteiner T 1990 *J. Phys.: Condens. Matter* **2** 8427
[7] Endo H, Tamura K and Yao M 1987 *Can. J. Phys.* **65** 266
[8] Tamura K and Inui M 2001 *J. Phys.: Condens. Matter* **13** R337
[9] Enderby J E and Barnes A C 1990 *Rep. Prog. Phys.* **53** 85
[10] Kikegawa T and Iwasaki H 1983 *Acta Crystallogr.* B **39** 158

[11] Keller R, Holzapfel W B and Schulz H 1977 *Phys. Rev.* B **16** 4404
[12] Takemura K, Mimomura S, Shimomura O, Fujii Y and Axe J D 1982 *Phys. Rev.* B **26** 998
[13] Young D A 1991 *Phase Diagrams of the Elements* (Berkeley, CA: University of California Press)
[14] Hanfland M, Schwarz U, Syassen K and Takemura K 1999 *Phys. Rev. Lett.* **82** 1197
[15] Rapoport E 1967 *J. Chem. Phys.* **46** 2891
[16] Brown K H and Barnett J D 1972 *J. Chem. Phys.* **57** 2009
[17] Tsuji K, Shimomura O, Tamura K and Endo H 1988 *Z. Phys. Chem., NF* **156** 495
[18] Tsuji K, Yaoita K, Imai M, Shimomura O and Kikegawa T 1989 *Rev. Sci. Instrum.* **60** 2425
[19] Brazhkin V V, Popova S V and Voloshin R N 1997 *High Pressure Res.* **15** 267
[20] Umnov A G and Brazhkin V V 1994 *High Temp.–High Pressure* **25** 221
[21] Umnov A G and Brazhkin V V 1995 *High Pressure Res.* **13** 233
[22] Umnov A G, Brazhkin V V, Popova S V and Voloshin R N 1992 *J. Phys.: Condens. Matter* **4** 1427
[23] Brazhkin V V, Voloshin R N, Popova S V and Umnov A G 1991 *Phys. Lett.* A **154** 413
[24] Brazhkin V V, Voloshin R N and Popova S V 1990 *JETP Lett.* **50** 424
[25] Brazhkin V V, Voloshin R N, Popova S V and Umnov A G 1992 *J. Phys.: Condens. Matter* **4** 1419
[26] Brazhkin V V, Voloshin R N, Popova S V and Umnov A G 1992 *High Pressure Res.* **6** 363
[27] Aasland S and McMillan P F 1994 *Nature* **369** 633
[28] Poole P H, Grande T, Angell C A and McMillan P F 1997 *Science* **275** 322
[29] Mishima O and Stanley H E 1998 *Nature* **396** 329
[30] Mishima O, Calvert L D and Whalley E 1985 *Nature* **314** 76
[31] Poole P H, Sciortino F, Essmann U and Stanley H E 1992 *Nature* **360** 324
[32] Katayama Y, Mizutani T, Utsumi W, Shimomura O, Yamakata M and Funakoshi K 2000 *Nature* **403** 170
[33] Funamori N and Tsuji K 2002 *Phys. Rev.* B **65** 014105
[34] Funamori N and Tsuji K 2002 *Phys. Rev. Lett.* **88** 255508
[35] Mezouar M, Le Bihan T, Libotte H, Le Godec Y and Hausermann D 1999 *J. Synchrotron Radiat.* **6** 1115
[36] Funakoshi K 1997 *PhD Thesis* Tokyo Institute of Technology
[37] Yaoita K, Katayama Y, Tsuji K, Kikegawa T and Shimomura O 1997 *Rev. Sci. Instrum.* **68** 2106
[38] Katayama Y, Tsuji K, Oyanagi H and Shimomura O 1998 *J. Non-Cryst. Solids* **234** 93
Katayama Y, Shimomura O and Tsuji K 1999 *J. Non-Cryst. Solids* **250–252** 537
Katayama Y 2001 *J. Synchrotron Radiat.* **8** 182
[39] Katayama Y, Tsuji K, Chen J-Q, Koyama N, Kikegawa T, Yaoita K and Shimomura O 1993 *J. Non-Cryst. Solids* **156–158** 687
Katayama Y 1996 *High Pressure Res.* **14** 383
Katayama Y, Tsuji K, Kanda H, Nosaka H, Yaoita K, Kikegawa T and Shimomura O 1996 *J. Non-Cryst. Solids* **205–207** 451
[40] Katayama Y, Tsuji K, Shimomura O, Kikegawa T, Mezouar M, Martinez-Garcia D, Besson J M, Hausermann D and Hanfland M 1998 *J. Synchrotron Radiat.* **5** 1023
[41] Nakano K and Katayama Y 2001 unpublished
[42] Crichton W A, Vaughan G B M and Mezouar M 2001 *Z. Kristallogr.* **216** 417
[43] Katayama Y 2002 *J. Non-Cryst. Solids* **312** 8
[44] Bellissent R, Gergman C, Ceolin R and Gaspard J P 1987 *Phys. Rev. Lett.* **59** 661
[45] Morimoto Y, Kato S, Toda N, Katayama Y, Tsuji K, Yaoita K and Shimomura O 1998 *Rev. High Pressure Sci. Tech.* **7** 245
[46] Tsuji K 1995 *Elementary Processes in Dense Plasmas* ed S Ichimaru and S Ogata (New York: Addison-Wesley) p 317
[47] Ohatani M and Tsuji K 1999 unpublished
[48] Tsuji K, Katayama Y, Morimoto Y and Shimomura O 1996 *J. Non-Cryst. Solids* **205–207** 298
[49] Tsuji K, Yaoita K, Imai M, Mitamura T, Kikegawa T, Shimomura O and Endo H 1990 *J. Non-Cryst. Solids* **117/118** 72
[50] Takemura K, Christensen N E, Novikov D L, Syassen K, Schwarz U and Hanfland M 2000 *Phys. Rev.* B **61** 14399
[51] Shimojo F, Zempo Y, Hoshino K and Watabe M 1997 *Phys. Rev.* B **55** 5708
[52] Chihara J and Kahl G 1998 *Phys. Rev.* B **58** 5314
[53] Tsuji K 1990 *J. Non-Cryst. Solids* **117/118** 27
[54] Yaoita K, Imai M, Tsuji K, Kikegawa T and Shimomura O 1991 *High Pressure Res.* **7** 229
[55] Tsuji K and Ohtani M 2000 *Science and Technology of High Pressure* ed M H Manghani, W J Nellis and M F Nicol (Hyderabad: Universities Press) p 498
Mori T, Tsuji K and Funamori N 2000 unpublished

[56] Yaoita K, Tsuji K, Imai M, Kikegawa T and Shimomura O 1990 *High Pressure Res.* **4** 339
Yaoita K, Tsuji K, Katayama Y, Imai M, Chen J-Q, Kikegawa T and Shimomura O 1992 *J. Non-Cryst. Solids* **150** 25
[57] Katayama Y, Mizutami T, Utsumi W, Shimomura O and Tsuji K 2001 *Phys. Status Solidi* b **223** 401
[58] Mori T, Tsuji K and Funamori N 2000 unpublished
Tsuji K and Ohtani M 2000 *Science and Technology of High Pressure* ed M H Manghani, W J Nellis and M F Nicol (Hyderabad: Universities Press) p 514
[59] Tsuji K and Katayama Y 1998 *The Physics of Complex Liquid* ed F Yonezawa, K Tsuji, K Kaji, M Doi and T Fujiwara (Singapore: World Scientific) p 83
[60] Yaoita K, Tsuji K, Katayama Y, Koyama N, Kikegawa T and Shimomura O 1993 *J. Non-Cryst. Solids* **156–158** 157
[61] Buentempo U, Filipponi A, Martinez-Garcia D, Postorino P, Mezouar M and Itie J P 1998 *Phys. Rev. Lett.* **80** 1912
[62] Gaspard J P, Marinelli F and Pellegatti A 1987 *Europhys. Lett.* **3** 1095
[63] Bichara C, Pellegatti A and Gaspard J P 1993 *Phys. Rev.* B **47** 5002
[64] Peck D R 1971 *Mellor's Comprehensive Treatise on Inorganic and Theoretical Chemistry, Phosphorus* vol VIII, Suppl. III (London: Longman) p 149
[65] Zhao Y, Von Dreele R B, Weidner D J and Schiferl D 1997 *High Pressure Res.* **15** 369
[66] Le Godec Y, Martinez-Garcia D, Mezouar M, Syfosse G, Iti J-P and Besson J-M 2000 *High Pressure Res.* **17** 35
[67] Clarke J H, Dore J C, Grande J R, Reed J and Walford G 1981 *Mol. Phys.* **42** 861
[68] Jovari P and Pusztai L 2002 *New Kinds of Phase Transformations: Transformations in Disordered Substances* ed V V Brazhkin, S V Buldyrev, V N Ryzhov and H E Stanley (New York: Kluwer) p 267
[69] Mizutani T, Katayama Y, Utsumi W, Funakoshi K, Yamakata M and Shimomura O 2000 *Science and Technology of High Pressure* ed M H Manghnani, W J Nellis and M F Nicol (Hyderabad: Universities Press) p 525
[70] Solozhenko V L and Peun T 1997 *J. Phys. Chem. Solids* **58** 1321
[71] Akahama Y, Utsumi W, Endo S, Kikegawa T, Iwasaki H, Shimomura O, Yagi T and Akimoto S 1987 *Phys. Lett.* A **122** 129
[72] Marani A and Guarise G B 1968 *Chimica Industria* **50** 663
[73] Hohl D and Jones R O 1994 *Phys. Rev.* B **50** 17047
[74] Morishita T 2001 *Phys. Rev. Lett.* **87** 105701
[75] Senda Y, Shimojo F and Hoshino K 2002 *J. Phys.: Condens. Matter* **14** 3715
[76] Morishita T 2002 *Phys. Rev.* B **66** 054204
[77] Sanloup C, Guyot F, Gillet P, Fiquet G, Hemely R J, Mezouar M and Martinez I 2000 *Europhys. Lett.* **52** 151
[78] Hattori T, Taga N, Takasugi Y, Mori T and Tsuji K 2002 *J. Phys.: Condens. Matter* **14** 10517
[79] Hattori T, Taga N, Takasugi Y, Mori T and Tsuji K 2002 *J. Non-Cryst. Solids* **312–314** 26
[80] Crichton W, Mezouar M, Grande T, Stolen S and Grzechnik 2001 *Nature* **414** 622
[81] Katayama Y and Inamura Y 2003 *J. Phys.: Condens. Matter* **15** S343